# High-power, Fused Assemblies Enabled by Advances in Fiber-Processing Technologies

## *Invited Paper*

Robert Wiley, Brett Clark

3SAE Technologies, Inc., 318 Seaboard Lane, Suite 212, Franklin, TN 37067, USA

rwiley@3sae.com

## ABSTRACT

The power handling capabilities of fiber lasers are limited by the technologies available to fabricate and assemble the key optical system components. Previous tools for the assembly, tapering, and fusion of fiber laser elements have had drawbacks with regard to temperature range, alignment capability, assembly flexibility and surface contamination. To provide expanded capabilities for fiber laser assembly, a wide-area electrical plasma heat source was used in conjunction with an optimized image analysis method and a flexible alignment system, integrated according to mechatronic principles. High-resolution imaging and vision-based measurement provided feedback to adjust assembly, fusion, and tapering process parameters. The system was used to perform assembly steps including dissimilar-fiber splicing, tapering, bundling, capillary bundling, and fusion of fibers to bulk optic devices up to several mm in diameter. A wide range of fiber types and diameters were tested, including extremely large diameters and photonic crystal fibers. The assemblies were evaluated for conformation to optical and mechanical design criteria, such as taper geometry and splice loss. The completed assemblies met the performance targets and exhibited reduced surface contamination compared to assemblies prepared on previously existing equipment. The imaging system and image analysis algorithms provided *in situ* fiber geometry measurement data that agreed well with external measurement. The ability to adjust operating parameters dynamically based on imaging was shown to provide substantial performance benefits, particularly in the tapering of fibers and bundles. The integrated design approach was shown to provide sufficient flexibility to perform all required operations with a minimum of reconfiguration.

**Keywords:** Splice, Taper, Bundle, Cleave, 3SAE, Glass Processing, Fusion, Ring of Fire, PCF Splice, Fiber laser

## 1. INTRODUCTION

The advancement of the state of the art of fiber laser technology has been quite rapid over the past decade. The increasing availability of efficient, powerful pump laser diodes and the development of pump combiner devices and attendant optical matching components has pushed attainable output power and radiance to previously unseen levels [1,2]. However, the tools for constructing such devices have not kept pace. Assembly of high-power fiber lasers and their components has remained a skilled craft, requiring lengthy manual processes and delivering low production yields.

Due to the high optical power levels involved, and especially with the development of cladding-pumped designs, the requirements for alignment, cleave quality, cleanliness, and correct splice, taper, and diffusion geometry are more stringent than even the most critical of previous lower-power applications. Cleave angle specifications for 125µm telecom splices typically allow 1° or more of deviation from the perpendicular, compared to a high power splice which might require <0.25° on fibers which are more challenging to cleave. Optical losses of 0.1dB, which might be acceptable for a splice in a telecom EDFA, will dissipate over 20W in a kilowatt laser, causing explosive failure of the splice [2]. The assembly process may require various tapering and diffusion procedures, as well as precision splicing, to create combiners and mode field adapters. These tapers must have correct adiabatic core geometry and in some cases a surface free of contaminants, which if left unchecked can cause destructive "hot spots" at high powers.

In the 1990's, several manufacturers introduced fiber preparation and fusion splicing machines that enabled the high-volume production of EDFA's for the telecom boom. These machines employed varying degrees of fixturing and automation to drastically reduce the time and skill required to make low-loss, high-strength splices. However, by design these tools were limited to relatively small fibers, typically 250μm maximum cladding diameter. Before these developments, hand alignment under optical microscopes and flame heat sources were the means used to splice fibers, just as they often are for the large diameter fibers of today's laser applications. [3]

As fiber lasers begin to move from R&D to volume production, there is a need to simplify, improve, and automate the steps required for their assembly, as was done for telecom applications. New cleaving and heat source technologies, implemented in a well designed workstation, comprise a substantial step forward in making high power laser manufacturing a high-yield, repeatable process. Flexible capabilities, including multi-axis positioning, wide field optics, and multi-application control software enable splicing, bundling, tapering, cleaving, and end-cap attachment to be performed on the same machine.
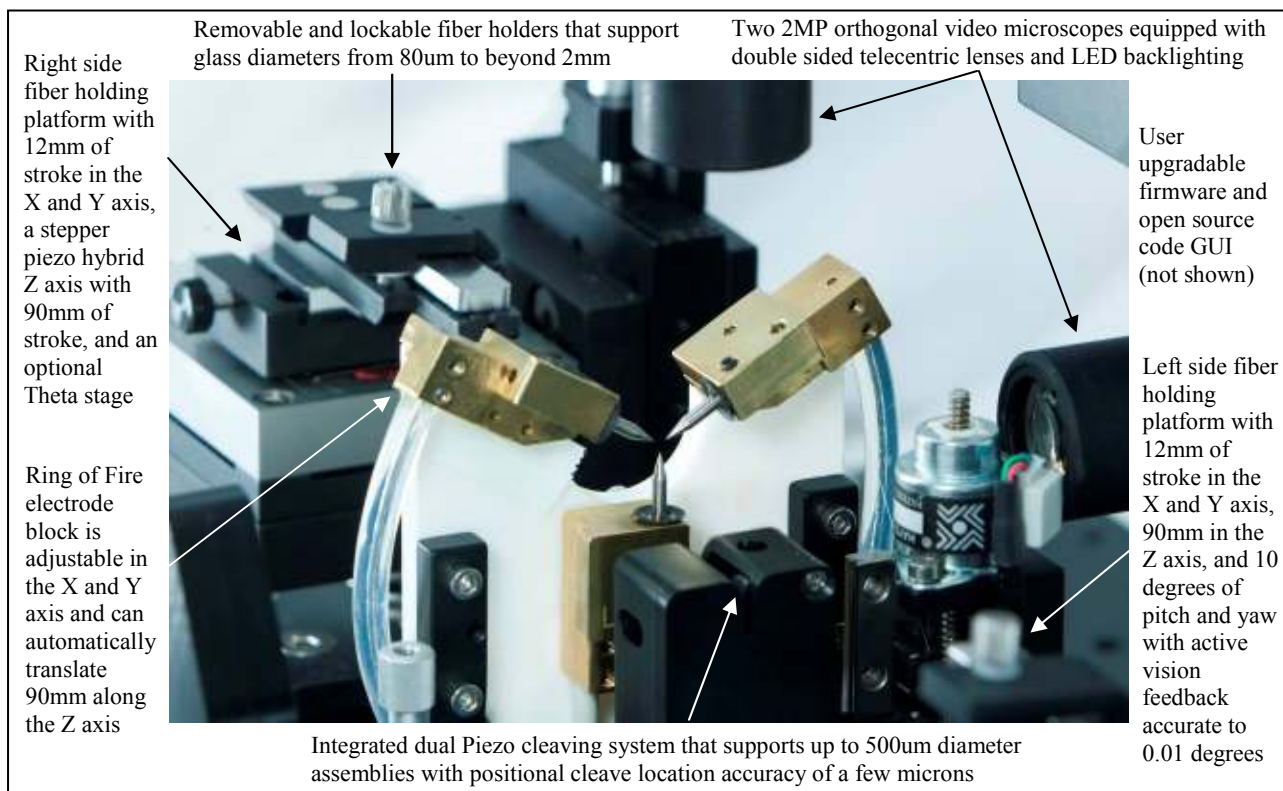


Right side fiber holding platform with 12mm of stroke in the X and Y axis, a stepper piezo hybrid Z axis with 90mm of stroke, and an optional Theta stage

Removable and lockable fiber holders that support glass diameters from 80um to beyond 2mm

Two 2MP orthogonal video microscopes equipped with double sided telecentric lenses and LED backlighting

User upgradable firmware and open source code GUI (not shown)

Left side fiber holding platform with 12mm of stroke in the X and Y axis, 90mm in the Z axis, and 10 degrees of pitch and yaw with active vision feedback accurate to 0.01 degrees

Ring of Fire electrode block is adjustable in the X and Y axis and can automatically translate 90mm along the Z axis

Integrated dual Piezo cleaving system that supports up to 500um diameter assemblies with positional cleave location accuracy of a few microns

Fig. 1 Large Diameter splicing System (LDS) from 3SAE Technologies, Inc. and some of its key features

## 2. HEAT SOURCE CONSIDERATIONS

Conventional arc fusion machines utilize a high voltage glow discharge between two electrodes, forming a heat source substantially in the shape of a narrow cylinder perpendicular to the fiber and only a few 10's of microns wide. Such heat sources are ineffective for larger fibers, because of the inability to heat all sides of the fiber equally. [4]

Flame and filament machines can be optimized to provide substantially circumferential heating, but they also extend the heat zone a relatively large distance along the fiber axis. This is advantageous for some operations, such as Thermally Expanded Core splicing (TEC), but causes substantial limitations in the geometries that can be spliced and formed. For example, these heat sources are poorly suited for splicing a small diameter fiber to a much larger fiber or optical device

(end cap, lens, prism). The heat required to raise the larger target to splicing temperatures will typically destroy the smaller fiber.

A multi-electrode plasma discharge is advantageous for these operations, as the resulting heat zone is isothermic around the circumference of the fiber, but relatively narrow in the axial direction. This allows for directed heating of larger or higher melting point portions of the assembly. With this system, accurately aligned, mechanically sound splices of small (80-125μm) fibers to very large (>2mm) fibers can be performed without difficulty. This is useful for attachment of fibers to end caps or bulk optic lenses.
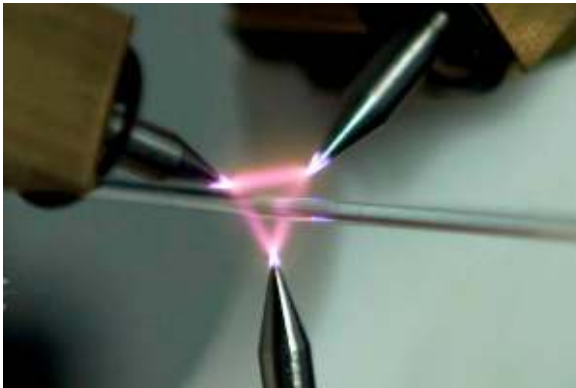


Fig. 2 "Ring of Fire®" plasma discharge
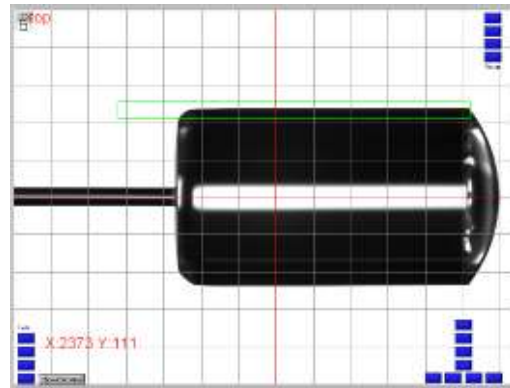


Fig. 3 End cap splice

## 3. CLEAVING TECHNOLOGY ADVANCEMENTS

The quality of fiber cleave angles is important for all fiber splicing, but especially so for large diameter fibers in high-power applications. [5,3] Cleave quality is primarily determined by three factors: scribe accuracy, correct fiber tension, and prevention of torsional strain (twist) in the tensioned fiber. Of these, the torsional strain problem is the most difficult to solve in a practical cleaving apparatus. Even very small rotational displacement between the two clamped points will produce unacceptable cleave angles. Traditionally, solutions to this have consisted of careful kinematic design of the fiber clamps, and the employment of relatively long distances (100mm or more) between the clamp points. As the effect on cleave angle is proportional to twist angle per unit length, a larger distance between the clamps ameliorates the effect of non-zero twist at the clamp mechanisms. This presents substantial inconvenience in many cases, however, when the length of accessible fiber is short. Furthermore, fibers with non-round cladding are particularly difficult to clamp without excess twist, even with optimized mechanical clamp designs.

Two new methods of providing fiber tension for cleaving with negligible twisting strain have been developed. The first is an *in situ* cleaver, operating on fibers still within the splice and tapering station (see Fig.1). The workstation was provided with a scribing device, incorporating a diamond blade positionable by a piezoelectric bending actuator and a stepper motor. The fiber positioning stages are of sufficiently rigid design that the Z-axis motion of the stages can be used to achieve tensions sufficient for even very large diameter fibers (>50N). A loadcell incorporated into one stage provides feedback for accurate control of the tension. Following a tapering or splicing operation, fibers, capillaries, or bundled fibers can be tensioned without twisting strain, since the strain will have been released during the time the fiber was softened by the heating process. In addition to the prevention of fiber twist, this system realizes additional advantages. The possibility of damage in transferring the tapered fiber or fibers to an external cleaver is prevented. The vision system of the workstation can be used to accurately locate the cleave point relative to known points on the fiber assembly. The accuracy and repeatability of this operation is much better than can be obtained from a system requiring mechanical indexing between the splice/taper station and an external cleaver. Optical assemblies of multiple short segments of dissimilar fiber can be conveniently and accurately made without removing the assembled side from the unit until completion. This reduces the risk of damage to the assembly and allows fixturing and fine alignment of the workpiece to be maintained throughout all operations.

For cleaving of fibers before a splicing operation, a cleaver using a second method of torsionless clamping has been developed. One clamp is conventional in design, with clamping force adjustable to suit different fiber diameters. The second clamp is implemented as a small reservoir of a low-melting-point alloy (LMA) which can be readily melted or solidified with a Peltier-junction device. The alloy used is free of lead and cadmium and is fully molten at less than 100°C. The fiber is "clamped" by being placed in the molten alloy, which is then solidified by rapid cooling. Large-diameter (>400μm) fibers, including shaped fibers, can be clamped without induced torsional strain. The cleaver has an inter-clamp distance of less than 60mm, as it does not depend on a large tensioned length to reduce torsion. The average cleave angle for a variety of round fibers is 0.16° (see Fig.4). The average angle for 500μm octagonal fiber is 0.22°. A 250μm PM fiber yielded an average of 0.33°. The higher angles for the PM fiber are believed to be due to the internal stresses induced by the PM structure. The Liquid Clamp Cleaver II (LCC II) is also configurable to create angled cleaves by automatically rotating the solidified clamp with an integrated stepper motor.
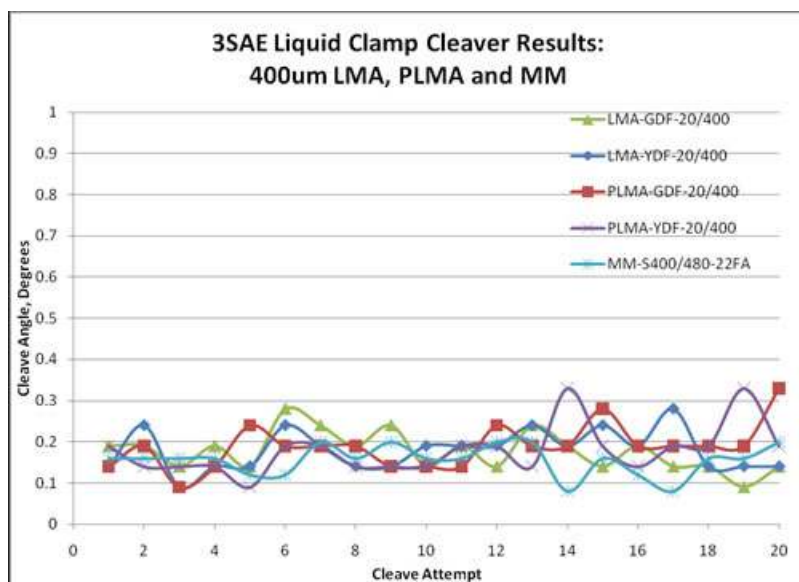


Fig. 4 Liquid Clamp Cleaver (LCC) from 3SAE Technologies, Inc. with 400um test data

Some large-diameter fibers, such as PM and PCF fibers, have internal structures that prevent smooth propagation of a cleaving fracture across the fiber. [5] In this case, a polishing operation may instead be used to provide a flat endface for splicing. An orbital polishing device with successive diamond paper grits of 30μm, 9μm, 3μm, and optionally 1μm has been used with good success for this purpose.

## 4. SPLICE QUALITY ASSESSMENT

The methods used for evaluating splice optical quality in single-mode fibers transfer poorly to the high power, large core, "few mode" application. The modal characteristics and beam quality of the test light source must match those of the actual application, or the "measured loss" result will be highly misleading. Furthermore, spatially concentrated losses, such as contamination "hot spots", can result in splice failure at dB levels far below that which would be acceptable from more spatially diffuse losses such as mode field mismatch. Such "hot spots" can cause explosive destruction of the splice, with consequential damage to pump lasers and associated equipment. In double-clad gain fibers, contamination must be prevented both at the fiber core and on the inner cladding surface (the outer cladding is typically fluoropolymer and must be removed for splicing). [2] The heating source used for splicing can be a contributor to fiber contamination, if particles of tungsten from a filament or electrodes are deposited during the operation. If such contamination occurs, a surface etch with HF may be required to restore the fiber surface.

A thermal infrared image inspection of the splice at operating power provides the most reliable and application specific indicator of splice quality. Figure 5 shows thermal infrared images of splices made using the "Ring of Fire®" three electrode system on polished 500µm fibers. No etching was used. 850W of pump laser power was applied at 915nm. Note the absence of local heating in the splice region, showing that neither the polishing nor splicing processes caused contamination of the splice region. The characteristics of three-electrode arc discharge will force any local contamination to follow the ion path around the fiber instead of impacting and contaminating the glass surface. Little or no tungsten / tungsten oxide deposition occurs when the system is operated with optimal electrode spacing and clean electrode surfaces.
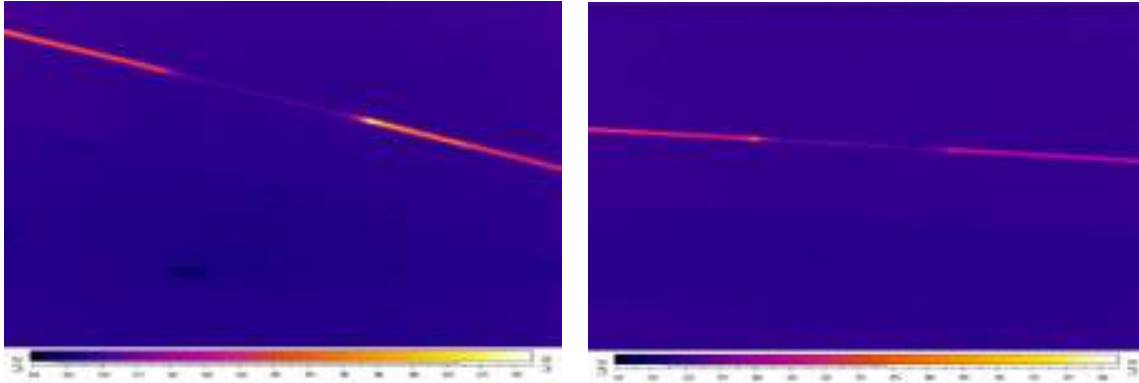


Fig. 5 FLIR images of un-etched 500um splices at 850W

## 5. TAPERING PERFORMANCE AND FIBER BUNDLING

The three-electrode system may also be used for the creation of adiabatic tapers in single fibers or fiber bundles. With fiber motions provided by long-travel micro stepping stages, a wide variety of taper geometries can be obtained.

The width of the heat source has a direct impact on the way in which tapers can be formed. Early work in tapering was done with flame or laser sources which provided a heat zone width (along the fiber axis) of many times the fiber diameter. The fiber motion was a simple bi-directional pull, yielding a taper geometry that was primarily a function of the heat distribution. [6,7] A more controllable method is to use a narrower heat source (axial length of heat zone similar to fiber diameter or less) and provide programmable motions and accelerations of the fiber and/or heat source. [8]

In such a system, one side of the fiber is in motion away from the heat source at a time-varying speed $V_1$, while the other moves towards the heat source at a lower speed $V_2$ (which may be fixed or variable). The cross sectional area of the fiber passing through the heated zone is reduced in the ratio of the two speeds:

$$\frac{A_{Original}}{A_{Taper}} = \frac{V_2}{V_1}$$

The "waist" diameter of the taper (minimum diameter) as a fraction of the original fiber diameter determines the desired final speed ratio:

$$\frac{V_{1Final}}{V_2} = \left(\frac{D_{Original}}{D_{Minimum}}\right)^2$$

The acceleration curve of $V_1$ determines the shape of the taper slope. Assuming a fixed $V_2$, a linear change in diameter over length is obtained by:

$$V_1 = V_2 \left( \frac{L}{(L-X) + X \left( \dfrac{D_{Minimum}}{D_{Original}} \right)} \right)^2$$

Where

$V_1$ = Speed of "pull" side of fiber
$V_2$ = Speed of "feed" side of fiber (fixed in this case)
$L$ = Length of taper
$X$ = Relative position of "pull" side, defined between $X$=0 (start) and $X$=$L$ (finish)

For high-ratio tapers, the ratio of the "fast" motor speed to the "slow" motor speed can be quite large. For example, to taper a 1mm fiber to 100µm would require a 100:1 ratio of speeds. Since the maximum speed is ultimately limited by motor performance, the starting and "feed" side motor speed ($V_2$) must be selected appropriately. If the required speed is very low, the initial part of the taper can take an excessive amount of time to complete. In this case, it is possible to begin with $V_1$ and $V_2$ at an intermediate speed, from which $V_1$ is accelerated and $V_2$ is decelerated to their final ratio of speeds. Although the speed calculations are more intensive, the improvement in process time can be 4:1 or more.

The width of the heat zone determines the accuracy with which the actual taper shape conforms to the geometry defined by the fiber velocity ratio. [8] A wider heat source, such as a flame or filament, causes additional non-linear curvature at the beginning and end of the linear taper. The three-electrode plasma heat source is substantially planar, with a narrow distribution along the fiber axis, resulting in a close conformation to the ideal behavior of the taper algorithm. If curved termini to the taper are desired, the velocity profile can be altered with additional terms to yield the required shape.

A wider heat zone does have the advantage of averaging out small changes in the fiber velocities or heat zone position, which reduces variation in the diameter of the tapered zone. The "Ring of Fire®" heat source can be made to sweep rapidly back and forth along a short distance (for example, 1mm of travel at a rate of 5 Hz). This simulates the effect of a wider heat source, providing a wider pseudo-Gaussian heat zone. This method is effective on larger fibers (>~500µm), but for smaller fibers the fiber cools too rapidly between passes of the plasma field for the averaging effect to be effective. [3]

To evaluate the tapering performance of the workstation, 500 µm fibers were tapered to 420µm in a 20mm linear taper, with an additional 20mm length of fiber at the tapered diameter, terminated by a cleaved end. The adiabatic performance of the tapers was evaluated by measuring the power transmitted through an aperture as a function of NA. The results as shown in the graphs indicate that the three samples evaluated provided adiabatic performance, with 100% of the power emitted from the taper output remaining in the calculated NA of 0.5. Measurement of the taper insertion loss showed an average of 0.97%, which is well within the measurement reproducibility of 2%. To detect possible localized heating, the tapers were illuminated with 107W of input power, and a FLIR camera was used to inspect for heat rise. The average heating of the tapers was 0.023°C/W, with a single non-destructive "hot spot" of 0.065°C/W on one taper. These tapers were not etched, but showed heating performance comparable to HF-etched tapers performed using a filament source.
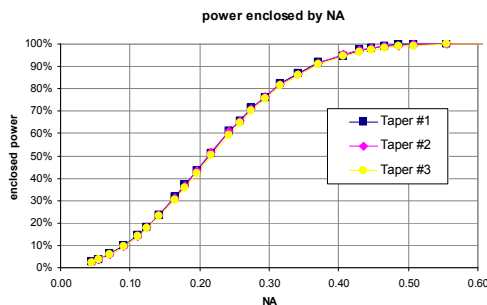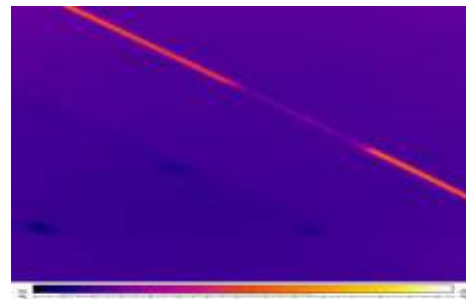


Fig. 6 Measured NA for 500um tapers



Fig. 7 FLIR image of 500um taper at 107W

As a secondary confirmation of performance particularly at high powers; a 10.5 (11.5 MFD)/200; 20 (18.5 MFD)/400 MFA was created by tapering the 400µm fiber to 220µm over 10mm. The taper was scanned to find the ideal cleave point based on matching the mode field profile of the tapered fiber to the output fiber. After the cleaving process, the input fiber was spliced on and over coated in lo-index recoat and potted. Once fully cured, 1-kW of signal was propagated through the core of the assembly. After several minutes, no measurable temperature increase was detected. Since a higher power source was not practical, power was intentionally injected into the cladding of the assembly using an offset splice to study the heating of a theoretical worst case assembly leaking 3% of the input power. The amount of cladding power and the temperature rise of the assembly is charted below. At 30W of cladding power (3% of 1000W) the forward temperature rise was 2.2°C. This correlates to 0.0022 °C/W for both the taper and the splice, assuming the said worst case 3% power leakage. Reversing the MFA (to study the impact of a strong back reflection) produced a temperature rise of 53.1°C (0.053°C/W) after ten minutes. The assembly had no detectable impact on the beam quality from either a $M^2$ (1.1) or a BPP perspective.
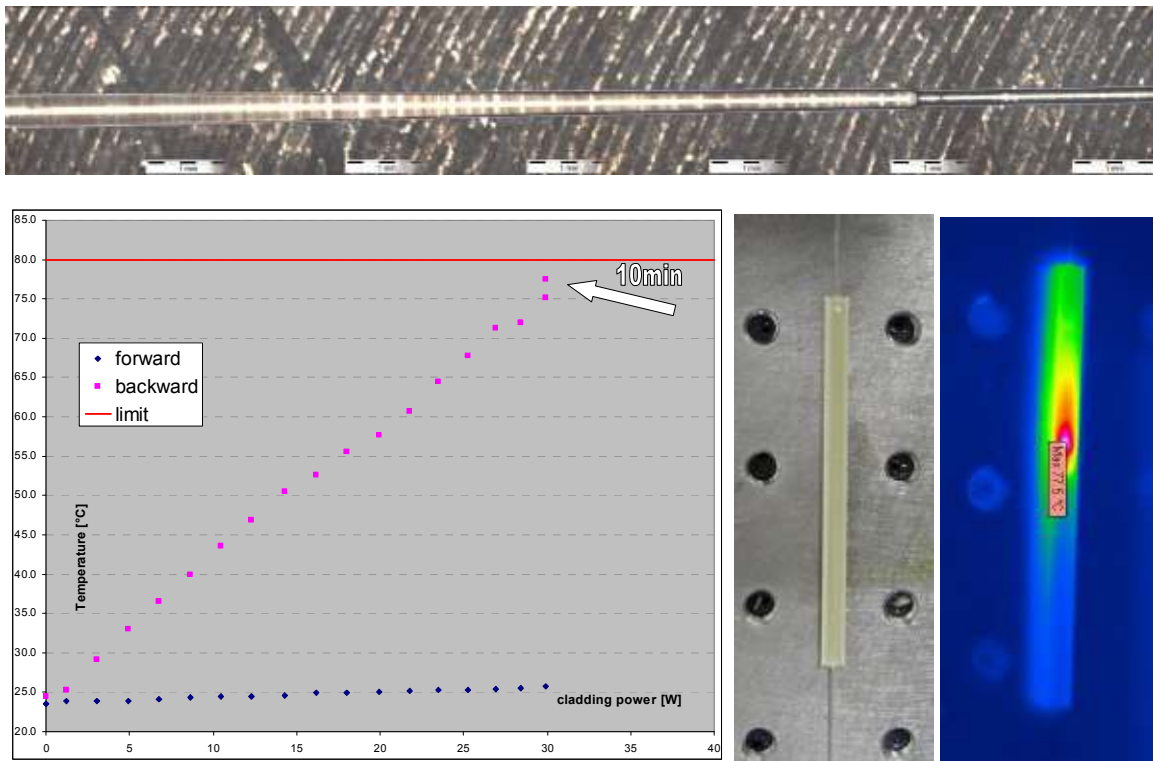




Fig. 8 Thermal dissipation tests of 10.5/200 to 20/400 MFA

Fabrication of tapered fiber bundles combines many of the fundamental techniques previously discussed. These techniques include adiabatic tapers, accurately located flat cleaves even with non-ideal glass structures, minimal surface contamination, precision thermal profile control, highly accurate vision system, and mechatronic controls. The additional steps required are pre-fusion fiber management techniques related to the application specific assembly of the device including, but not limited to, optimized pack ratio, minimizing signal fiber distortion, and controlling orientation of stress rods or other internal fiber structures. [4, 9] The performance criteria for tapered bundles are wide-ranging, application-specific, and typically proprietary information of system end-users. For these reasons, they are outside the scope of the present paper.
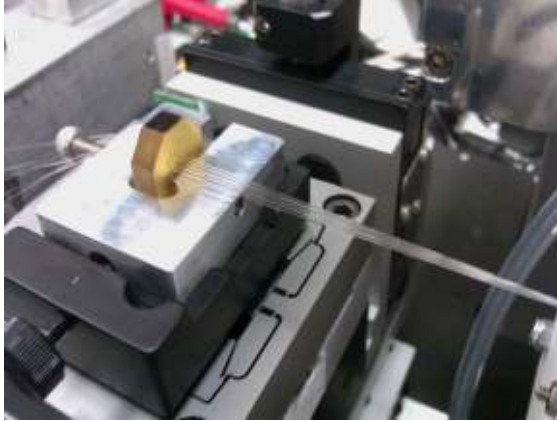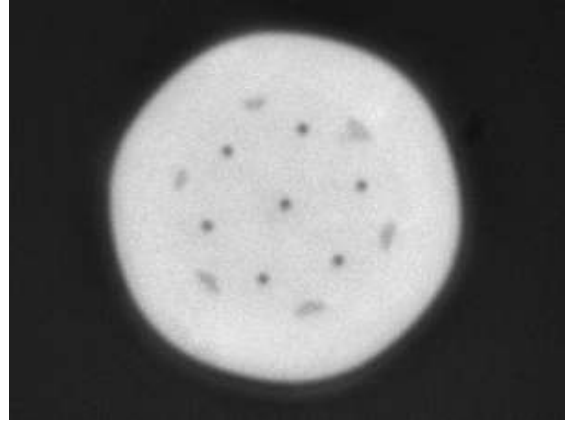
Fig. 9 Assembling a bundle without a capillary



Fig. 10 Cleaved end of 7:1 combiner, 40um OD

## 6. SPLICING PCF FIBERS

Photonic Crystal Fibers (PCF) are increasingly appearing in high-power fiber laser applications. Cleaving these fibers presents particular difficulties, due to their very fragile nature. Fusion splicing of PCF can result in a collapse of the fiber structure, causing large changes in the optical properties of the fiber near the splice. Optimized cleaving techniques can minimize fracturing for some PCF structures, but the more "holey" configurations are difficult to cleave by any method. [5,8]

For some applications such as end cap splicing, a subtle beam divergence caused by a short and well-controlled length of collapsed PCF structure can be tolerated. [5,10]This can enable improved cleaving of particularly difficult fibers, and improved mechanical strength of the splice. The axially narrow heat zone of the three-electrode system allows the fiber structure to be collapsed and solidified in a controlled way in a very short length of the fiber. Following an initial cleave, the roughly cleaved end of the PCF may be consolidated for a length of 200µm or less by application of the arc discharge. The now-solidified fiber end can then be polished to create a well-defined perpendicular end face, with a very short (<50µm for a 500µm fiber) collapsed zone. This can be spliced to conventional fibers with little or no additional increase in the collapsed length.

For applications in which no collapse of the fiber structure can be tolerated, the "Ring of Fire®" system enables a very controlled and rapid application of heat to the splice point. The outer cladding can be solidly fused before the temperature of the inner structure becomes sufficiently softened to deform. The resulting splices are less mechanically sound than those produced by partial collapse, but have superior optical guiding properties, with little or no disruption of the beam geometry. [11]
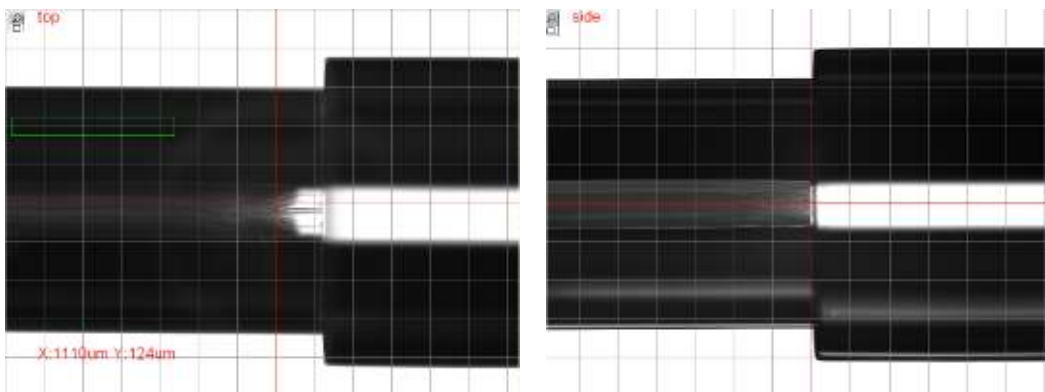


Fig. 11 PCF splices: Collapsed vs. uncollapsed.

# 7. VISION SYSTEM

The vision system is active during all operations of the workstation and can provide semi-automatic alignment of fibers for splicing and similar operations. A variety of automatic algorithms are provided to measure the geometry of tapers and splices, to determine fiber diameter, alignment, and symmetry.
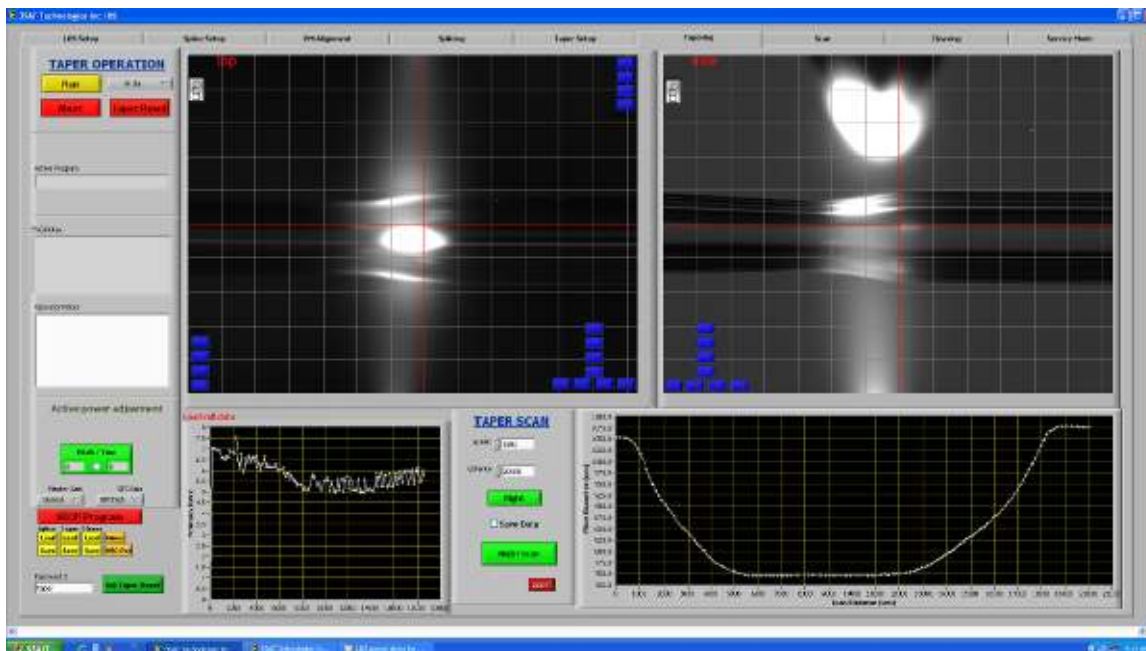


Fig. 12 Screen capture of GUI interface with vision system analyzing tapered capillary

The "Ring of Fire[®]" three-electrode system is near-isothermal across a large segment of the planar discharge, when considered as a heat source for splicing smaller diameter fibers. For larger diameter applications, it is necessary to properly center the fiber(s) in order to deliver uniform heating. This is particularly true of thin-wall capillaries which may be tapered, for example in the production of capillary-based combiners. These capillaries lack a strong conductive heat path across their diameter, and have a larger ratio of surface area to thermal mass. Therefore they are particularly sensitive to any variation in heating along their circumference. The vision system of the workstation can be effectively used to align the heat source by observing the brightness of the heated workpiece (as an indicator of local temperature) across the image in two orthogonal views. An improved method is to apply a constant taper elongation to a thin wall capillary passing though the heat source. The tension required to produce the taper will be minimized when the capillary is evenly heated on all sides. This allows the workstation to center the heat zone in an automated process.

# 8. A MORE VERSATILE HEAT SOURCE IN DEVELOPMENT

The "Ring of Fire[®]" heat source consists of a digitally-controlled three-phase high-voltage source driving three tungsten electrodes. The points of the electrodes form an equilateral triangle, and the resulting plasma discharge forms in a triangular shape about their mutual center and perpendicular to the fiber axis. The electrode spacing can be varied from 1mm to 3mm or more, depending on the desired transverse width of the heat zone. Closer spacing provides more stability at lower input power. Wider spacing provides even heating of larger fibers. The system can be adjusted from very low power (suitable for splicing of <80µm fibers) to a maximum of 150W of input power, which will easily splice and taper 2mm fibers and bundles. The effective width of the heat zone along the fiber axis varies with input power, from ~50µm to ~500µm.

Although the axially narrow heat zone of the three-phase "Ring of Fire[®]" has advantages for many applications, a broader heat source benefits applications such as Thermally Expanded Core splicing, post-splice fire polishing, and high

ratio tapers, For such applications, the three electrode system can be expanded to a six-electrode configuration ("Tunnel of Fire™"). In this system, a multiphase drive circuit forms a three-dimensional glow discharge, completely surrounding the fiber for a length of easily up to 5mm and possibly as large as 10mm. The two triangular sets of three electrodes can be aligned and driven 120° displaced in phase, or rotationally offset by 60° with their tips forming an irregular octahedron. The spacing between the two sets may be adjusted to control the axial extent of the plasma vortex. Electronic adjustments to the drive waveforms can significantly alter the heat distribution transferred to the fiber or device. This system can also be operated as one or two independent three-phase planar systems. Testing and application development of the plasma vortex system is ongoing.

With most conventional heat sources, including the "Ring of Fire®", the axial distribution of heat is essentially Gaussian, and the width of the effective heat zone can not be changed during operation. The six-electrode system opens new possibilities, as the heat distribution is controlled by the relative phase of different features of the drive waveforms, and can be altered asymmetrically and in real time. This will provide more flexible heat application for dissimilar-fiber splices and tapering. As described previously, for a narrow, symmetrical heat source, the geometry of a taper is defined by the motion and acceleration of the two segments of fiber on either side of the molten zone. A heat source with an axial extent of several millimeters and an asymmetrical heat zone can produce tapers defined by temperature distribution rather than acceleration. [6,7]
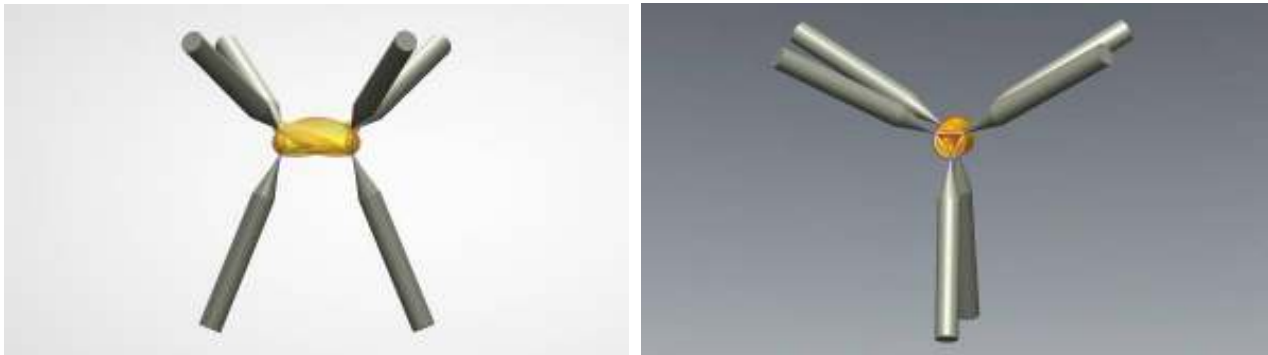


Fig. 13 A novel plasma heat source with a thermal profile controllable in 3 dimensions

## 9. CONCLUSIONS

To provide expanded capabilities for fiber laser assembly, a wide-area electrical plasma heat source was used in conjunction with an optimized image analysis method and a flexible alignment system, integrated according to mechatronic principles. High-resolution imaging and vision-based measurement provided feedback to adjust assembly, fusion, and tapering process parameters. The system was used to perform assembly steps including dissimilar-fiber splicing, tapering, bundling, capillary bundling, and fusion of fibers to large bulk optic devices. The completed assemblies met the performance targets and exhibited reduced surface contamination compared to assemblies prepared on previously existing equipment.

## 10. ACKNOWLEDGMENT

## 11.  REFERENCES

[1]  Z. Jihuang, "Ytterbium-doped High Power Fiber Lasers with Fused Fiber Bundle Combiner", Proc. SPIE **7276**, POEM 2008: Laser Technology and Applications, (2009)

[2]  F. Gonthier, et al., "High-power All-Fiber$^{®}$ components: The missing link for high power fiber lasers", ITF Optical Technologies Inc., St-Laurent (Quebec) Canada

[3]  D. Yablon, "Optical Fiber Fusion Splicing", Springer-Verlag, (2005)

[4]  B. S. Wang, E.W. Mies, "Review of Fabrication Techniques for Fused Fiber Components for Fiber Lasers", Proc. SPIE **7195**, Fiber Lasers VI: Technology, Systems, and Applications, (2009)

[5] NKT, Photonics, "Fiber Handling, Stripping, Cleaving and Coupling", Application Note V1.0, www.NKTphotonics.com, (2009)

[6]  D. R. Fairbanks, "Thermal visco-elastic simulation model for tapering of laser-heated silica fiber", Proc. SPIE **1580**, Fiber Optic Components and Reliability, (1991)

[7]  T. A. Birks, Y. W. Li. "The Shape of Fiber Tapers", Journal of Lightwave Technology, **10**, 432, (1992)

[8]  B. S. Wang, E.W. Mies, "Advanced Topics on Fusion Splicing of Specialty Fibers and Devices", Proc. SPIE **6781**, Passive Components and Fiber-based Devices, (2007)

[9]  C. Jauregui, "All-fiber Side Pump Combiner for High Power Fiber Lasers and Amplifiers", Proc. SPIE **7580**, Fiber Lasers VII: Technology, Systems, and Applications, (2007)

[10] J. Hecht, "Understanding Fiber Optics", 3$^{rd}$ Edition, Prentice Hall, (1999)

[11] NKT, Photonics, "Splicing Single Mode PCFs", Application Note V1.0, www.NKTphotonics.com, (2009)